J. Fluid Mech. (1995), *vol.* 285, *pp.* 69–94

On the identification of a vortex

By JINHEE JEONG AND FAZLE HUSSAIN
Department of Mechanical Engineering, University of Houston, Houston, TX 77204-4792, USA

(Received 6 December 1993 and in revised form 4 July 1994)

Considerable confusion surrounds the longstanding question of what constitutes a vortex, especially in a turbulent flow. This question, frequently misunderstood as academic, has recently acquired particular significance since coherent structures (CS) in turbulent flows are now commonly regarded as vortices. An objective definition of a vortex should permit the use of vortex dynamics concepts to educe CS, to explain formation and evolutionary dynamics of CS, to explore the role of CS in turbulence phenomena, and to develop viable turbulence models and control strategies for turbulence phenomena. We propose a definition of a vortex in an incompressible flow in terms of the eigenvalues of the symmetric tensor $\boldsymbol{S}^2+\boldsymbol{\Omega}^2$; here $\boldsymbol{S}$ and $\boldsymbol{\Omega}$ are respectively the symmetric and antisymmetric parts of the velocity gradient tensor $\nabla \boldsymbol{u}$. This definition captures the pressure minimum in a plane perpendicular to the vortex axis at high Reynolds numbers, and also accurately defines vortex cores at low Reynolds numbers, unlike a pressure-minimum criterion. We compare our definition with prior schemes/definitions using exact and numerical solutions of the Euler and Navier–Stokes equations for a variety of laminar and turbulent flows. In contrast to definitions based on the positive second invariant of $\nabla \boldsymbol{u}$ or the complex eigenvalues of $\nabla \boldsymbol{u}$, our definition accurately identifies the vortex core in flows where the vortex geometry is intuitively clear.

1. Introduction

The concept of vortices is as old as the subject of hydrodynamics; yet, an accepted definition of a *vortex* is still lacking. Turbulence is viewed as a tangle of vortex filaments, and much of turbulence physics is well explained using the concepts of vortex dynamics (e.g. see Tennekes & Lumley 1972; Hunt 1987). Turbulent shear flows have been found to be dominated by spatially coherent, temporally evolving vortical motions, popularly called *coherent structures* (CS) (Cantwell 1981; Lumley 1981; Hussain 1980). Vortex dynamics, which govern the evolution and interaction of CS and coupling of CS with background turbulence, is promising not only for understanding turbulence phenomena such as entrainment and mixing, heat and mass transfer, chemical reaction and combustion, drag, and aerodynamic noise generation, but also for viable modeling of turbulence (Hussain & Melander 1991). We must identify dynamically significant, large-scale vortical regions in turbulent flows as a necessary first step, which in turn necessitates an objective definition of a vortex.

Several conditional-sampling techniques have been suggested for CS eduction in experiments and numerical simulations (e.g. Mumford 1982; Blackwelder 1977; Fiedler & Mensing 1985; Ferré & Giralt 1989; Kim 1985; Hussain 1986). In transitional flows, eduction is relatively simple because transitional CS occur with detectable regularity in time and space. Hence, a reference signal such as velocity can be used as a trigger for eduction (Hussain & Zaman 1980; Cantwell & Coles 1983).

However, in fully developed turbulent flows, such as far-field regions of jets, wakes and mixing layers, instantaneous vorticity fields are necessary to infer the dynamical significance of vortical structures (Tso 1983; Tso & Hussain 1989; Hussain & Hayakawa 1987; Bisset, Antonia & Browne 1990). Unfortunately, even instantaneous vorticity fields are inadequate to reveal CS in turbulent boundary layers (Robinson 1991).

Intuitively, a vortex is often considered to be a tube whose surface consists of vortex lines (Lamb 1945, p. 202). However, the existence of a vortex tube does not imply the existence of a vortex; for instance, a vortex tube in a laminar pipe flow is not a vortex in any sense.

Specific definitions of a vortex have been recently proposed. Lugt (1979) defines a vortex as a 'multitude of material particles rotating around a common center'. According to Chong, Perry & Cantwell (1990), a vortex is a region of *complex eigenvalues* of $\nabla \boldsymbol{u}$, while Hunt, Wray & Moin (1988) identify a vortex as a region containing *both a positive second invariant of* $\nabla \boldsymbol{u}$ *and low pressure*. These definitions will be discussed in more detail in §§2.2 and 3.

Using a DNS database, Robinson (1991) showed that the low-pressure criterion effectively captures vortical structures in a turbulent boundary layer. However, in general, an appropriate pressure level cannot be specified to identify all vortical regions in a flow. Also, in a mixing layer, pressure within the longitudinal ribs between large-scale spanwise rolls may not be sufficiently low, so that a single pressure threshold cannot reveal both ribs and rolls (see §2.1).

Recognizing that the size of a vortex in a viscous fluid depends on the identifier's threshold selected, we limit our interest here to the identification of vortex cores. Numerous studies suggest that the cores of vortical CS in turbulent flows are well localized in space.

We consider the following to be the requirements for a vortex core:

(i) A vortex core must have a net vorticity (hence, net circulation). Thus, potential flow regions are excluded from vortex cores, and a potential vortex is a vortex with zero cross-section.

(ii) The geometry of the identified vortex core should be Galilean invariant.

Unfortunately, these requirements do not result in a single identification scheme. Therefore, we will use these requirements only as a preliminary check of potential identification schemes. Our objective is to develop a scheme which identifies vortex cores in any flow. In this paper, we do not focus on the dynamical significance of vortices or CS, but only on their objective detection.

In the next section, we will show that intuitive definitions fail in many situations. The definitions of Chong *et al.* (1990) and Hunt *et al.* (1988) will be summarized in §3, and a new definition will be introduced in §4. Finally, in §5, previous definitions will be compared with ours using exact and numerical solutions of the Euler and Navier–Stokes equations. During comparison of various definitions, we will discuss our basis for preferring one definition over another.

2. Inadequacies of intuitive measures

In this section, we discuss that three common intuitive indicators of vortices – pressure minimum, closed or spiralling streamlines and pathlines, and isovorticity surface – are inadequate in detecting vortices in an unsteady flow in general.

2.1. *Local pressure minimum*

The physical reasoning for this criterion is that, in a vortex, pressure tends to have a local minimum on the axis of a circulatory or swirling motion when the centrifugal force is balanced by the pressure force (the so-called cyclostrophic balance), which is strictly true only in a steady inviscid planar flow. The concept of a local pressure minimum in three dimensions requires clarification because pressure may have a minimum in all directions at a point, or it may have a minimum only in a plane perpendicular to the vortex axis (e.g. Burgers vortex). Here, we will discuss the latter condition (i.e. minimum in a plane), which is less restrictive and may include the former case as well. This is related to Hunt *et al.*'s (1988) second condition, i.e. pressure in the core is lower than that near the vortex boundary.

A well-defined pressure minimum can exist in an unsteady irrotational motion which does not necessarily involve a vortex by the first requirement in §1. Consider an unsteady irrotational axisymmetric motion with a stagnation point: $u_r = -\alpha(t)\, r$, $u_\theta = 0$, and $u_z = 2\alpha(t)\, z$. Integrating the Euler equations, we find that pressure is

$$p = (\dot{\alpha} - \alpha^2)\tfrac{1}{2} r^2 + (-\dot{\alpha} - \alpha^2)\, z^2,$$

where $\dot{\alpha}$ is the time derivative of the strain rate $\alpha(t)$. When $\dot{\alpha} - \alpha^2 > 0$, pressure has a local minimum in any (r, θ)-plane, even though the flow has no vorticity, nor even swirl, and hence, there is no vortex core. This pressure minimum is a simple consequence of the unsteady strain rate $\alpha(t)$. Even in a steady flow, there is a well-known exception where the centrifugal force is balanced not by the pressure force but by the viscous force: Kármán's viscous pump. In this case, the centrifugal force does not affect the radial pressure distribution, which is constant in planes perpendicular to the vortex axis. Another counter example is Stokes flow (at very low *Re*), where the pressure gradient is balanced only by the viscous term, so that pressure satisfies the Laplace equation. From the minimum principle for this equation, it follows that a local pressure minimum is impossible in planar Stokes flows, while vortices can occur (e.g. viscous vortex near a sharp corner (Moffatt 1963) and vortices in front of and behind a step (Panton 1984, p. 641)). In addition, planar irrotational flows such as sink or source flows have a pressure minimum at the origin but involve no swirl whatsoever. Thus, the existence of a local pressure minimum is neither a sufficient nor a necessary condition for the presence of a vortex core in general.

Since pressure is governed by the Poisson equation, $\nabla^2 p = -\rho u_{i,j} u_{j,i}$ (here the subscript comma denotes partial differentiation, and the summation convention is used for indices), pressure is inherently of a larger scale than vorticity. For example, in a Lamb vortex (a decaying axisymmetric vortex from an initial line vortex; see Lamb 1945, p. 592) (see figure 1*a*), vorticity nearly vanishes (to 1.8% of maximum) at $r = 4(\nu t)^{1/2}$, while pressure still has a significant value ($\sim 25\%$ of the maximum negative value). In a Burgers vortex (a steady rectilinear vortex in an axisymmetric strain field; this vortex undergoes axisymmetric stretching due to the irrotational strain rate, the stretching being balanced by the diffusion of vorticity; see Batchelor 1967, p. 272), where the lengthscale of vorticity (and thus the lengthscale of the vortex core) is fixed, the lengthscale of the pressure hump, i.e. the radius of the $\partial p/\partial r = 0$ point (figure 1*b*) increases with the value of the vorticity on the axis. This inherent scale difference between a vortex core and the associated low-pressure region makes the demarcation of vortices, using an isopressure surface, problematic. For example, in a mixing layer, an isopressure surface fails to capture ribs and rolls simultaneously (see figure 1*c*; compare with the corresponding isovorticity surface shown in figure 7*e*). If a lower

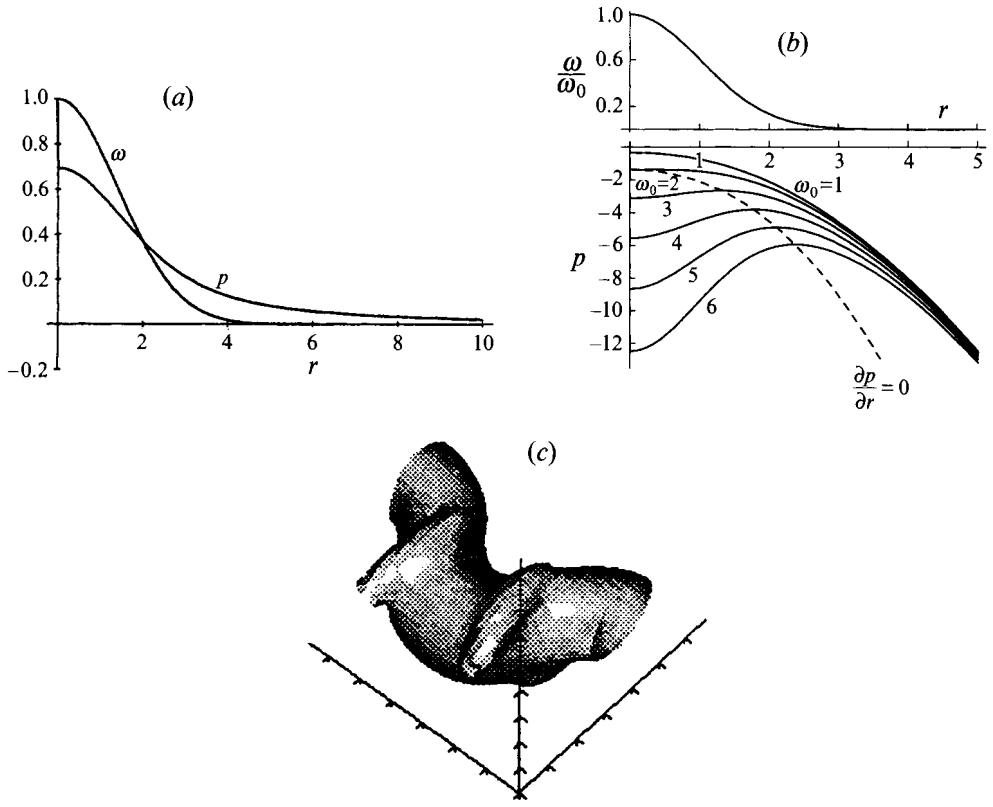

FIGURE 1. (*a*) Pressure and vorticity distributions in a Lamb vortex. (*b*) Pressure and vorticity distributions in a Burgers vortex; ω_0 is the vorticity at the vortex centre. (*c*) Isopressure surface in a mixing layer.

pressure level is used to capture the ribs, the isopressure surface extends far outside the rolls and fails to provide any clear indication of rolls; the pressure within the ribs is nearly the ambient value and is much higher than that at the roll centre.

2.2. *Pathline and streamline*

Lugt (1979) proposed the use of closed or spiral pathlines to detect vortices. However, a pathline obviously fails to satisfy requirement (ii) in § 1. Another critical inadequacy of this definition is that a particle may not complete a full revolution around the vortex centre (hence no closed pathline) during the lifetime of a vortex. This occurs when vortices undergo transition due to nonlinear processes such as pairing, tearing, core dynamics or breakdown before fluid particles in the vortex can undergo a full revolution. Also, in regions of reconnection (Melander & Hussain 1988), especially at high *Re*, pathlines and streamlines can be highly contorted because of the rapidly transforming vortex line topology. Even in an optimal reference frame, these interacting regions of vortices, which remain – and may even become more – dynamically significant during reconnection, would escape identification.

The use of closed or spiral streamlines as a definition of a vortex is equally problematic beause they also are not Galilean invariant. This is illustrated in figure 2(*a–c*), which shows streamline patterns of an axisymmetric vortex in three different reference frames. Similarly, figure 2(*d–f*) shows velocity vector patterns measured during early stages of roll pairing in an axisymmetric jet (Hussain & Zaman 1980).

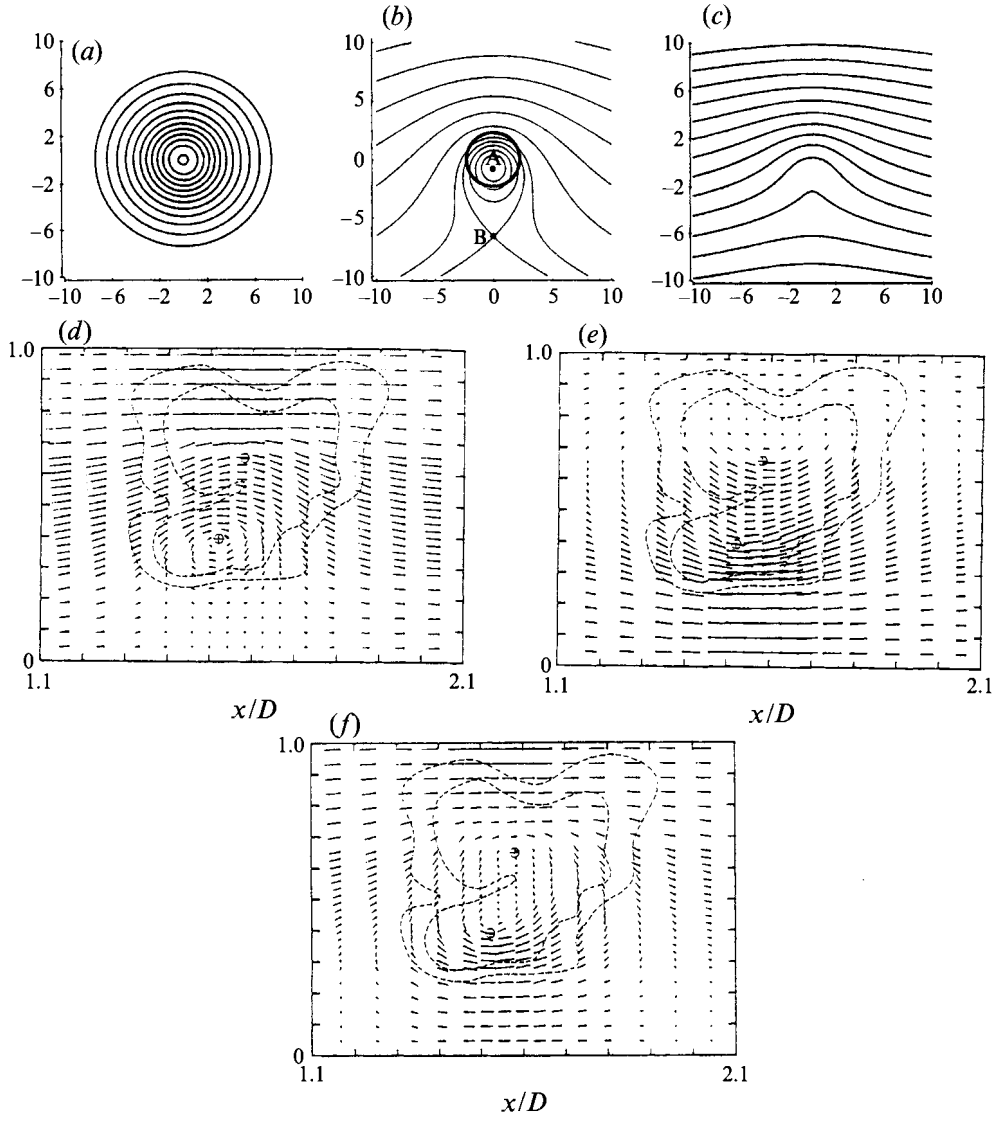

FIGURE 2. (*a–c*) Streamlines of a Lamb vortex in different reference frames, moving: (*a*) with the vortex centre; (*b*) with a point within the core; and (*c*) faster than any point. (*d–f*) Distribution of velocity vectors in the near field of an axisymmetric jet with a reference frame velocity of: (*d*) $1.25U_e$ (convection velocity of lower vortex); (*e*) $0.35U_e$ (convection velocity of upper vortex); and (*f*) $0.8U_e$ (the average of the convection velocities of the two vortices). Dotted lines represent structure boundary based on vorticity magnitude.

Thus, this definition will obscure two or more vortices moving at different speeds in any single reference frame and will surely fail in a turbulent flow containing numerous vortices advecting at different speeds.

2.3. *Vorticity magnitude*

Vorticity magnitude ($|\omega|$) has been widely used to educe CS and represent vortex cores (Metcalfe *et al.* 1985; Hussain & Hayakawa 1987; Bisset *et al.* 1990). However, this approach, though fairly successful in the free shear flows investigated so far, may not

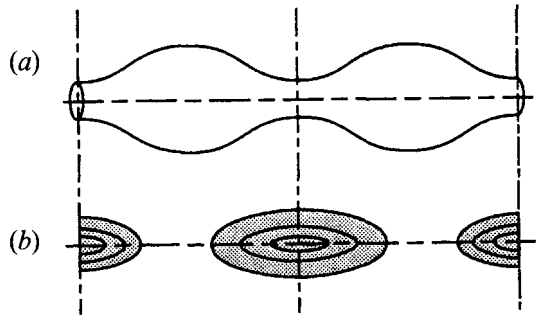

FIGURE 3. Axisymmetric vortex with an axial variation in vorticity: (*a*) vortex surface, (*b*) vorticity surface.

always be satisfactory since $|\omega|$ does not identify vortex cores in a shear flow, especially if the background shear is comparable to the vorticity magnitude within the vortex. An example is a streamwise vortex embedded in a homogeneous shear flow (see §5.2). Also, in planar wall-bounded flows, Lugt (1979) showed that the maxima and minima of $|\omega|$ occur only at the wall. In a turbulent boundary layer, the maximum $|\omega|$ occurs near the high-speed streak regions (Jimenez *et al.* 1988). However, in both cases, the flow immediately near the wall is characterized by shear, but by no means exhibits a swirling (i.e. vortical) motion. Thus, since a vortex core must exclude a wall, $|\omega|$ is not a suitable criterion for vortex identifiation in a boundary layer.

Even in free shear flows, there are potential difficulties in identifying vortices from $|\omega|$ surfaces. For instance, a vorticity sheet is not a vortex even though it may have a large vorticity magnitude. Another counter example is an axisymmetric vortex with a strong axial variation in vorticity, i.e. with strong core dynamics (Melander & Hussain 1993), in which a $|\omega|$ surface may terminate along the vortex axis (see the schematic in figure 3) indicating segmented vortices although there is only one continuous vortex column.

Thus, a $|\omega|$ surface at a sufficiently low level is necessary but not sufficient to detect a vortex in both free and wall-bounded free shear flows. Detailed examples of the potential misrepresentation of vortices by $|\omega|$ are given in §5.2.

3. Previously proposed definitions

Recently, two distinct Galilean-invariant definitions of a vortex have been proposed using invariants of the velocity gradient tensor (Chong *et al.* 1990; Hunt *et al.* 1988; Melander & Hussain 1993). We review these definitions briefly in this section.

3.1. *Complex eigenvalues of velocity gradient tensor*

Chong *et al.* (1990) used eigenvalues of the velocity gradient tensor $\nabla \boldsymbol{u}$ to classify the local streamline pattern around any point in a flow in a reference frame moving with the velocity of that point (i.e. a critical point). They proposed that a vortex core is a region with complex eigenvalues of $\nabla \boldsymbol{u}$; complex eigenvalues imply that the local streamline pattern is closed or spiral in a reference frame moving with the point.

The eigenvalues, σ, of $\nabla \boldsymbol{u}$ satisfy the characteristic equation

$$\sigma^3 - P\sigma^2 + Q\sigma - R = 0,$$

where $P \equiv u_{i,i} = 0$ (incompressible flow), $Q \equiv \frac{1}{2}(u_{i,i}^2 - u_{i,j}u_{j,i}) = -\frac{1}{2}u_{i,j}u_{j,i}$ and $R =$

$\mathrm{Det}(u_{i,j})$ are the three invariants of $\nabla \boldsymbol{u}$. Complex eigenvalues will occur when the discriminant (Δ) is positive, i.e.

$$\Delta = (\tfrac{1}{3}Q)^3 + (\tfrac{1}{2}R)^2 > 0. \tag{1}$$

Note that this definition, derived from $\nabla \boldsymbol{u}$, is Galilean invariant.

The physical interpretation of this definition is provided by considering the streamlines of a Lamb vortex in a moving reference frame (figure 2*b*). In the reference frame moving with particles A and B, both of which have the same velocity, a closed streamline pattern appears around A within the vortex core (marked by a thick line) that denotes positive Δ, and a saddle occurs at B outside the vortex core where Δ is negative.

3.2. *The second invariant of* $\nabla \boldsymbol{u}$ *and kinematic vorticity number* N_k

Hunt *et al.* (1988) defined an 'eddy' as the region with positive second invariant, Q, of $\nabla \boldsymbol{u}$, with the additional condition that the pressure be lower than the ambient value. The second invariant Q is defined as

$$Q \equiv \tfrac{1}{2}(u_{i,i}^2 - u_{i,j}u_{j,i}) = -\tfrac{1}{2}u_{i,j}u_{j,i} = \tfrac{1}{2}(\|\boldsymbol{\Omega}\|^2 - \|\boldsymbol{S}\|^2), \tag{2}$$

where $\|\boldsymbol{S}\| = [\mathrm{tr}(\boldsymbol{S}\boldsymbol{S}^t)]^{1/2}$, $\|\boldsymbol{\Omega}\| = [\mathrm{tr}(\boldsymbol{\Omega}\boldsymbol{\Omega}^t)]^{1/2}$, and $\boldsymbol{S}$ and $\boldsymbol{\Omega}$ are the symmetric and antisymmetric components of $\nabla \boldsymbol{u}$; i.e. $S_{ij} = \frac{1}{2}(u_{i,j} + u_{j,i})$ and $\Omega_{ij} = \frac{1}{2}(u_{i,j} - u_{j,i})$. Thus, Q represents the local balance between shear strain rate and vorticity magnitude.

It can be easily shown that Q vanishes at a wall, unlike $|\omega|$; i.e. shear strain and vorticity have the same magnitude at a stationary wall. The most general velocity gradient at the wall is given by

$$\nabla \boldsymbol{u} = \begin{pmatrix} 0 & 0 & a \\ 0 & 0 & b \\ 0 & 0 & 0 \end{pmatrix},$$

which gives $Q = 0$ at the wall. Note that this necessarily implies $\Delta = 0$, since $R = 0$ at the wall. Therefore, definitions based on Δ and Q are free from the problem associated with $|\omega|$, which fails to properly represent vortical motion near a wall (see §2.3). However, as will be shown later, in spite of this advantage, definitions based on Δ and Q are not helpful in certain situations.

Truesdell (1953, p. 107) introduced the kinematic vorticity number N_k to measure 'the quality of rotation', instead of the local rotation rate given by $\|\boldsymbol{\Omega}\|$. He defined N_k as

$$N_k \equiv \left(\frac{|\omega|^2}{2S_{ij}S_{ij}}\right)^{1/2} = \frac{\|\boldsymbol{\Omega}\|}{\|\boldsymbol{S}\|} = \left(1 + \frac{2Q}{S_{ij}S_{ij}}\right)^{1/2}. \tag{3}$$

Thus, N_k is a pointwise measure of $|\omega|$ non-dimensionalized by the norm of the strain rate, which gives the quality of rotation regardless of the vorticity magnitude. For example, $N_k = \infty$ and $N_k = 0$ correspond to solid-body rotation and irrotational motion respectively, regardless of the $|\omega|$ value. In their study of vortex core dynamics, Melander & Hussain (1993) identified the core of an axisymmetric vortex column as 'a maximally connected spatial region with $N_k > 1$'. It is easy to see from (3) that *a region with* $N_k > 1$ *is identical to that with* $Q > 0$. However, since N_k is non-dimensionalized by the magnitude of strain rate, the peak N_k value is oblivious of the dynamical significance of a vortex. In other words, N_k does not discriminate between vortices with small and large vorticity (or circulation) as long as the quality of rotation is the same for both.

Q can also be interpreted as the source term of pressure in the Navier–Stokes equations. From the Poisson equation for pressure ($\nabla^2 p = 2\rho Q$) and the maximum principle, we conclude that the pressure maximum occurs only on the boundary if $Q > 0$, and the pressure minimum occurs only on the boundary if $Q < 0$ (Truesdell 1953). However, $Q > 0$ does not necessarily imply that the pressure minimum occurs within the region; i.e. the pressure minimum can occur on the boundary of the region of $Q > 0$. Thus, there is no explicit connection between a region with $Q > 0$ and a region of a pressure minimum. In this sense, the definitions used by Hunt *et al.* (1988) and Melander & Hussain (1993) are not strictly identical, even though in most situations they turn out to be equivalent.

From (1), it is obvious that the condition $Q > 0$ is more restrictive than $\Delta > 0$, although which definition is more appropriate is not clear *a priori*.

4. New definition

Although a pressure minimum cannot be used as a general detection criterion for a vortex core, as shown in §2.1, it provides a starting point for a new definition. The inconsistency between the existence of a pressure minimum and the existence of a vortex core arose in §2.1 due to two effects: (i) unsteady straining, which can create a pressure minimum without involving a vortical or swirling motion, and (ii) viscous effects, which can eliminate the pressure minimum in a flow with vortical motion. By simply discarding these effects, we expect to obtain a better indicator for the existence of a vortex. Since information on local pressure extrema is contained in the Hessian ($p_{,ij}$) of pressure, let us consider the equation for $p_{,ij}$. Taking the gradient of the Navier–Stokes equations, we find

$$a_{i,j} = -\frac{1}{\rho} p_{,ij} + \nu u_{i,jkk}, \tag{4}$$

where $a_{i,j}$ is the acceleration gradient, and $p_{,ij}$ is symmetric. Then, $a_{i,j}$ can be decomposed into symmetric and antisymmetric parts as follows:

$$a_{i,j} = \underbrace{\left[\frac{\mathrm{D}S_{ij}}{\mathrm{D}t} + \Omega_{ik}\Omega_{kj} + S_{ik}S_{kj}\right]}_{\text{symmetric}} + \underbrace{\left[\frac{\mathrm{D}\Omega_{ij}}{\mathrm{D}t} + \Omega_{ik}S_{kj} + S_{ik}\Omega_{kj}\right]}_{\text{antisymmetric}}. \tag{5}$$

The antisymmetric part of (4) is the well-known vorticity transport equation. The symmetric part of (4) is

$$\frac{\mathrm{D}S_{ij}}{\mathrm{D}t} - \nu S_{ij,kk} + \Omega_{ik}\Omega_{kj} + S_{ik}S_{kj} = -\frac{1}{\rho} p_{,ij}. \tag{6}$$

The occurrence of a local pressure minimum in a plane requires two positive eigenvalues of the tensor $p_{,ij}$. Here, as argued above, we will not consider the contributions of the first two terms in the left-hand side of (6) since the first term represents unsteady irrotational straining and the second term represents viscous effects. Thus, we consider only $\boldsymbol{S}^2 + \boldsymbol{\Omega}^2$ to determine the existence of a local pressure minimum due to vortical motion and *define a vortex core as a connected region with two negative eigenvalues of* $\boldsymbol{S}^2 + \boldsymbol{\Omega}^2$. Note that since $\boldsymbol{S}^2 + \boldsymbol{\Omega}^2$ is symmetric, it has real eigenvalues only. If λ_1, λ_2 and λ_3 are the eigenvalues and $\lambda_1 \geqslant \lambda_2 \geqslant \lambda_3$, the new definition is equivalent to the requirement that $\lambda_2 < 0$ within the vortex core.

λ_1	λ_2	λ_3	$\Sigma\lambda_i$	Negative λ_2	Positive Q
+	−	−	−	vortex core	vortex core
+	−	−	+	vortex core	not vortex core
+	+	−	−	not vortex core	vortex core
+	+	+	+	not vortex core	not vortex core

TABLE 1. Possible choices of eigenvalues and the differences of the definitions based on positive Q and on negative λ_2

From (2) and (5),

$$Q = -\tfrac{1}{2}\nabla\cdot\boldsymbol{a} = -\tfrac{1}{2}\mathrm{tr}\,(\boldsymbol{S}^2+\boldsymbol{\Omega}^2) = -\tfrac{1}{2}(\lambda_1+\lambda_2+\lambda_3)$$

(see also Truesdell 1953, p. 79). Then, Q can be interpreted as an average of the balance between $\langle \boldsymbol{x}, \boldsymbol{S}^2\boldsymbol{x}\rangle/\langle \boldsymbol{x},\boldsymbol{x}\rangle$ and $\langle \boldsymbol{x}, \boldsymbol{\Omega}^2\boldsymbol{x}\rangle/\langle \boldsymbol{x},\boldsymbol{x}\rangle$ in all directions because

$$Q = -\tfrac{1}{2}\mathrm{tr}\,(\boldsymbol{S}^2+\boldsymbol{\Omega}^2) = -\frac{3}{2A}\int\frac{\langle \boldsymbol{x}, (\boldsymbol{S}^2+\boldsymbol{\Omega}^2)\,\boldsymbol{x}\rangle}{\langle \boldsymbol{x},\boldsymbol{x}\rangle}\,\mathrm{d}A,$$

where the integration is over the surface of an infinitesimal sphere surrounding a given point, A is the surface area of the infinitesimal sphere, and $\langle\,,\rangle$ denotes an inner product.

Unlike the definition based on positive Q, we require the balance of $\langle \boldsymbol{x}, \boldsymbol{S}^2\boldsymbol{x}\rangle$ and $\langle \boldsymbol{x}, \boldsymbol{\Omega}^2\boldsymbol{x}\rangle$ in only one eigenplane. Since $\langle \boldsymbol{x}, \boldsymbol{S}^2\boldsymbol{x}\rangle \geqslant 0$, while $\langle \boldsymbol{x}, \boldsymbol{\Omega}^2\boldsymbol{x}\rangle \leqslant 0$, our new definition requires $|\langle \boldsymbol{x}, \boldsymbol{\Omega}^2\boldsymbol{x}\rangle|$ to be greater than $\langle \boldsymbol{x}, \boldsymbol{S}^2\boldsymbol{x}\rangle$ in one eigenplane of $\boldsymbol{S}^2+\boldsymbol{\Omega}^2$. As $\boldsymbol{S}^2+\boldsymbol{\Omega}^2$ vanishes at a wall, the new definition excludes the possibility of a vortex core centred at a wall. Thus, this definition with a single condition, in essence, incorporates features of Hunt *et al.*'s (1988) two separate conditions by considering only vortical contributions to local pressure minima. However, these two definitions do not necessarily agree; this is clearly illustrated in §5.4, where we establish the superiority of our definition.

4.1. *Some estimates of eigenvalues of* $\boldsymbol{S}^2+\boldsymbol{\Omega}^2$

Recall that, of the eigenvalues $\lambda_1 \geqslant \lambda_2 \geqslant \lambda_3$ of $\boldsymbol{S}^2+\boldsymbol{\Omega}^2$, since $\langle \boldsymbol{x}, \boldsymbol{S}^2\boldsymbol{x}\rangle \geqslant 0$ and $\langle \boldsymbol{x}, \boldsymbol{\Omega}^2\boldsymbol{x}\rangle \leqslant 0$, the largest eigenvalue λ_1 satisfies

$$\sigma_1^2 = \max\frac{\langle \boldsymbol{x}, \boldsymbol{S}^2\boldsymbol{x}\rangle}{\langle \boldsymbol{x},\boldsymbol{x}\rangle} \geqslant \max\frac{\langle \boldsymbol{x}, (\boldsymbol{S}^2+\boldsymbol{\Omega}^2)\,\boldsymbol{x}\rangle}{\langle \boldsymbol{x},\boldsymbol{x}\rangle} = \lambda_1 \geqslant \min\frac{\langle \boldsymbol{x}, \boldsymbol{S}^2\boldsymbol{x}\rangle}{\langle \boldsymbol{x},\boldsymbol{x}\rangle} = \sigma_3^2,$$

where $\sigma_1^2 \geqslant \sigma_2^2 \geqslant \sigma_3^2$ are eigenvalues of $\boldsymbol{S}^2$ (see Courant & Hilbert 1953, p. 31). The smallest eigenvalue λ_3 is

$$\lambda_3 = \min\frac{\langle \boldsymbol{x}, (\boldsymbol{S}^2+\boldsymbol{\Omega}^2)\,\boldsymbol{x}\rangle}{\langle \boldsymbol{x},\boldsymbol{x}\rangle} \geqslant \min\frac{\langle \boldsymbol{x}, \boldsymbol{\Omega}^2\boldsymbol{x}\rangle}{\langle \boldsymbol{x},\boldsymbol{x}\rangle} = -\tfrac{1}{4}|\boldsymbol{\omega}|^2.$$

To summarize, $\sigma_1^2 \geqslant \lambda_1 \geqslant \sigma_3^2$ and $\lambda_2 \geqslant \lambda_3 \geqslant -\frac{1}{4}\omega^2$. We list the possible choices of eigenvalues and the differences of the two definitions based on positive Q and negative λ_2 (i.e. negative definite $\boldsymbol{S}^2+\boldsymbol{\Omega}^2$ in one eigenplane) in table 1.

4.2. *Equivalence of definitions in planar flow*

In planar flows, the regions defined by the following conditions are equivalent:

(i) negative λ_2; λ_2 is the second largest eigenvalue of $\boldsymbol{S}^2+\boldsymbol{\Omega}^2$;

(ii) complex eigenvalues of $\nabla \boldsymbol{u}$;
(iii) positive Q.

To verify this statement, consider a general velocity gradient for a planar flow:

$$\nabla \boldsymbol{u} = \begin{pmatrix} a & b \\ c & -a \end{pmatrix}.$$

The characteristic equation for eigenvalues σ of $\nabla \boldsymbol{u}$ is $\sigma^2 + Q = 0$, where $Q = -a^2 - bc$. Thus, $\sigma = \pm(-Q)^{1/2}$. Hence, condition (iii) is the same as condition (ii). Also,

$$\boldsymbol{S}^2 + \boldsymbol{\Omega}^2 = \begin{pmatrix} a^2+bc & 0 \\ 0 & a^2+bc \end{pmatrix}.$$

Thus, negative λ_2 requires that $a^2 + bc < 0$, i.e. $Q > 0$. Therefore, these three definitions are equivalent for planar flows.

5. Applications of definitions

In this section, the definitions discussed in §§2.3 and 3–4 will be evaluated and compared using exact solutions and DNS data. The prospective definitions of a vortex core to be analysed are summarized here for convenience.

(i) λ_2-definition: the region of negative λ_2; λ_2 is the second largest eigenvalue of $\boldsymbol{S}^2 + \boldsymbol{\Omega}^2$ (surfaces with $\lambda_2 = 0$ are excluded).

(ii) Δ-definition: the region of complex eigenvalues of $\nabla \boldsymbol{u}$. The boundary of this region is given by the surface

$$\Delta = (\tfrac{1}{3}Q)^3 + (\tfrac{1}{2}R)^2 = 0$$

(surfaces with $\Delta = 0$ are excluded).

(iii) Q-definition: the region of positive $Q = \frac{1}{2}(\|\boldsymbol{\Omega}\|^2 - \|\boldsymbol{S}\|^2) = -\frac{1}{2}(\lambda_1 + \lambda_2 + \lambda_3)$; $\lambda_1 \geqslant \lambda_2 \geqslant \lambda_3$ are eigenvalues of $\boldsymbol{S}^2 + \boldsymbol{\Omega}^2$ (surfaces with $Q = 0$ are excluded). In all examples considered, Hunt *et al.*'s (1988) additional condition for low pressure is found to be automatically satisfied. Thus, the Q-definition is equivalent to Hunt *et al.*'s definition for the examples considered in the following.

(iv) $|\omega|$-definition: the region of vorticity magnitude greater than a certain threshold. Note that the $|\omega|$-definition is subjective, since it requires an arbitrary threshold on $|\omega|$.

We will evaluate these four definitions in flows where the vortex geometry is intuitively clear. In this way, we will justify our λ_2-definition by demonstrating its success in flows where the other definitions are clearly inadequate. Many analytic examples and DNS databases have been tested, and only examples with significant differences are presented and discussed.

5.1. *Interpretation of Δ-, λ_2- and Q-definitions in axisymmetric flows*

Flows in this class have circular streamlines in an inertial frame moving with the centre regardless of the azimuthal velocity profile. Since the flow is planar, the three definitions are the same, as shown in §4.2. In cylindrical coordinates, the velocity field can be written in general as

$$u_r = u_z = 0, \quad u_\theta = V(r, t).$$

Therefore,

$$\boldsymbol{S}^2 + \boldsymbol{\Omega}^2 = \begin{pmatrix} -VV'/r & 0 & 0 \\ 0 & -VV'/r & 0 \\ 0 & 0 & 0 \end{pmatrix},$$

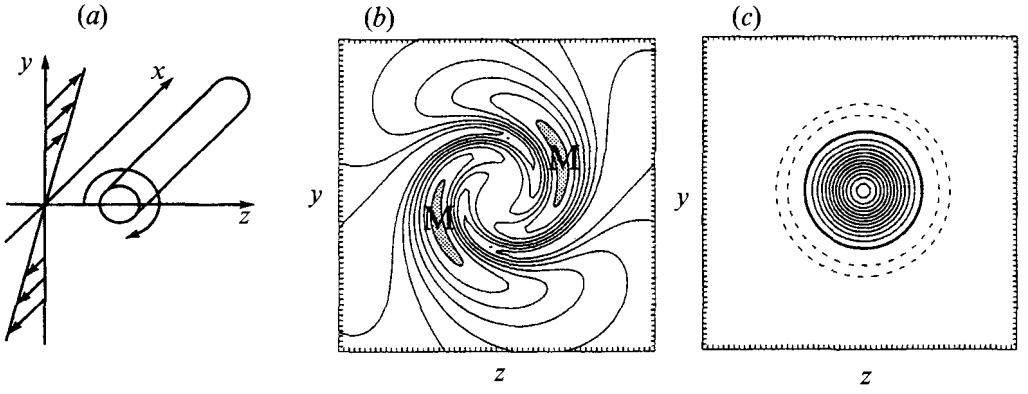

FIGURE 4. (*a*) Schematic of an inviscid streamwise vortex in a homogeneous shear flow. (*b*) Contours of $|\omega|$; 'M' denotes locations of maximum $|\omega|$. (*c*) Contours of $-\lambda_2$.

where $V' = \partial V/\partial r$. For negative λ_2, it is necessary that $VV' > 0$; i.e. $\partial V^2/\partial r > 0$. Thus, according to each definition, a vortex core is the region where the azimuthal velocity magnitude increases from the centre with increasing radius. Since

$$\omega_z = \frac{1}{r}\frac{\partial r u_\theta}{\partial r},$$

ω_z is positive as long as $u_\theta = O(1/r^{1-\alpha})$ with $\alpha \geqslant 0$, as is commonly the case. Therefore, the $|\omega|$-definition requires an arbitrary cutoff to define a vortex core; however, the Δ-, Q- and λ_2-definitions clearly identify the boundary of the vortex core as the radial location of maximum u_θ (i.e. $\partial V^2/\partial r = 0$).

5.2. *Inadequacy of the $|\omega|$-definition*

5.2.1. *An inviscid streamwise vortex in a homogeneous shear flow*

As sketched in figure 4(*a*), this vortex can be considered as an idealization of a streamwise vortical structure in a flat-plate turbulent boundary layer (this is a typical structure in the wall region; see Jeong 1994). The equation of motion for streamwise velocity (u) is decoupled from the equations for vertical (v) and spanwise (w) velocities as follows:

$$\left.\begin{aligned} \frac{\partial u}{\partial t} + v\frac{\partial u}{\partial y} + w\frac{\partial u}{\partial z} &= 0, \\ \frac{\partial v}{\partial t} + v\frac{\partial v}{\partial y} + w\frac{\partial v}{\partial z} &= -\frac{1}{\rho}\frac{\partial p}{\partial y}, \\ \frac{\partial w}{\partial t} + v\frac{\partial w}{\partial y} + w\frac{\partial w}{\partial z} &= -\frac{1}{\rho}\frac{\partial p}{\partial z}. \end{aligned}\right\} \tag{7}$$

The velocities v and w do not change in time when the streamwise vorticity is constant along a streamline in a (y,z)-plane. For instance, $\omega_x = f(r)$, where $r = (y^2+z^2)^{1/2}$, so that u is advected by v and w. Thus, a closed-form solution is easily obtained for a vortex with an initial Gaussian vorticity distribution, $\omega_x = 2\exp(-r^2)$, superimposed by a uniform background shear $u(y) = Sy$. That is,

$$u = Sr\sin\left(\frac{(1-\mathrm{e}^{-r^2})t}{r^2} + \theta\right), \quad v = -\frac{(1-\mathrm{e}^{-r^2})z}{r^2}, \quad w = \frac{(1-\mathrm{e}^{-r^2})y}{r^2},$$

where $\theta = \tan^{-1}(y/z)$.

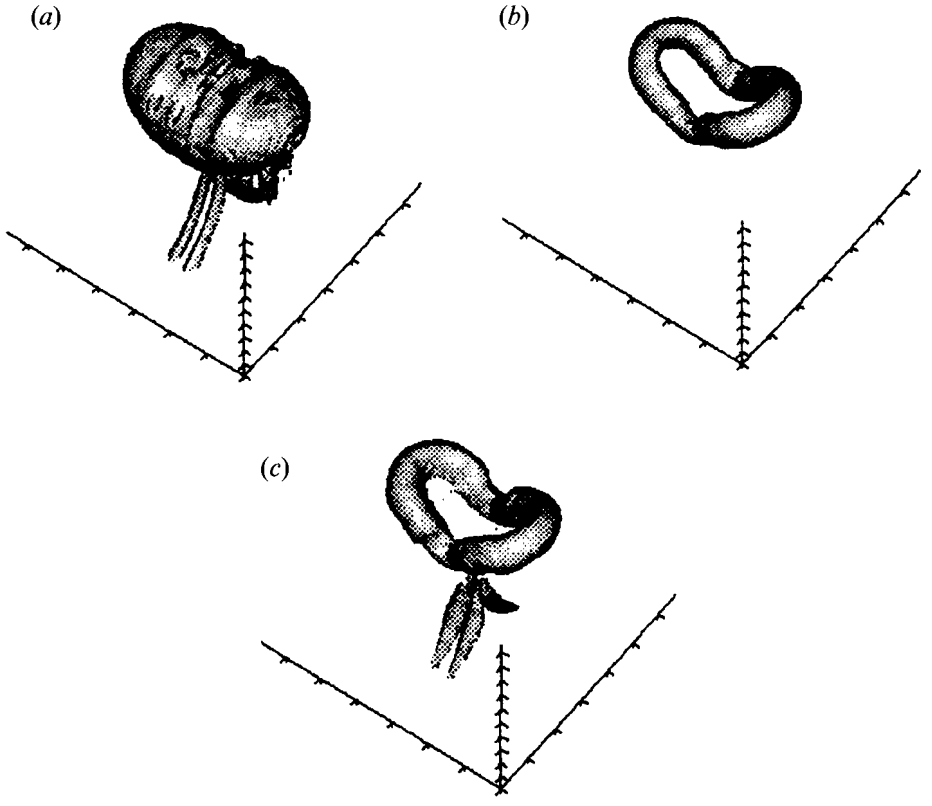

FIGURE 5. Surfaces of: (a) $|\omega| = 0.1\%$ of maximum; (b) $|\omega| = 30\%$ of maximum; and (c) $\lambda_2 = 0$ in an elliptic jet.

After the flow has evolved for some time, the $|\omega|$-definition eventually exhibits two disconnected peaks which are irrelevant to the vortex geometry (figure 4*b*). Furthermore, since $|\omega|$ changes shape and size with time, the $|\omega|$-definition is clearly inadequate, considering that the swirling motion of the streamwise vortex (i.e. v and w velocities) does not change in time. In contrast, the vortex core based on the λ_2-definition (figure 4*c*) is steady and shows one vortex core, consistent with the vortex geometry shown in figure 4(*a*).

This example, together with the fact that $|\omega|$ is always maximum at the wall of a (flat plate) boundary layer, is proof enough that the $|\omega|$-definition is inappropriate in wall layers. Next, we consider difficulties of the $|\omega|$-definition in a free shear flow.

5.2.2. *Elliptic vortex ring*

We consider DNS data for an elliptic vortex ring (see Husain & Hussain 1993), where two classes of vortices appear: an elliptic vortex ring with high $|\omega|$ and rib-like streamwise vortices with lower $|\omega|$ behind the elliptic ring. This configuration of vortices is particularly useful for our purpose since we can demonstrate in a realistic flow the inability of the $|\omega|$-definition to simultaneously represent vortices with a large variation in $|\omega|$. The low-level $|\omega|$ surface which reveals the rib vortices (figure 5*a*) does not clearly demarcate the elliptic vortex ring, and the $|\omega|$ surface which reveals the ring omits the ribs (figure 5*b*). In comparison, the λ_2-definition shows both the ring and ribs

clearly (figure 5*c*). Such a failure of a $|\omega|$-definition is expected in a variety of other free shear flows.

5.3. *Inadequacy of the Δ-definition*

5.3.1. *Conically symmetric vortex*

Here we consider a proposed model for a tornado (Shtern & Hussain 1993) consisting of a swirling jet emerging into a half-space with a source of axial momentum and circulation, located at the origin. The flow has a conical symmetry, satisfies the full Navier–Stokes equations, and has no singularity on the axis except at the origin (figure 6*a*). Since this flow has an axial velocity in addition to an azimuthal velocity around the vortex axis (the z-axis), it exhibits strong helical motion. The velocity field in spherical coordinates is

$$v_r = -\frac{\psi'(x)}{r}, \quad v_\theta = -\frac{\psi(x)}{r\sin\theta}, \quad v_\phi = \frac{\Gamma(x)}{r\sin\theta} \quad \text{and} \quad x = \cos\theta,$$

where r, θ and ϕ are the radius, angle from the axis and azimuthal angle in spherical coordinates. Since this flow has a conical symmetry, the vortex core boundary should also be conical in shape. Contour lines near the origin ($r = 0$) are excluded in the following because the velocity field is singular at the origin.

The Δ-definition shows two vortex cores marked by grey shading in figure 6(*b*): one (region 1) on the axis and another (region 2) detached from the axis, which is a misrepresentation of the vortex geometry. The presence of the detached region 2 can be explained as follows. Let us consider streamlines in the meridional flow (figure 6*c*). The velocities at points A and C are respectively larger and lower than that at point B, because the velocity increases as the origin is approached. When the reference frame moves with the point B (figure 6*d*), the local streamline pattern around B becomes closed (note that this is the meridional flow only). This yields a positive-Δ region detached from the actual vortex core. In contrast, $-\lambda_2$ is maximum and positive on the axis, without a spurious detached vortex core (figure 6*e*).

Since CS with core dynamics contain helical vortex lines and strong axial flow (Melander & Hussain 1993; Schoppa, Husain & Hussain 1993), the superiority of the λ_2-definition to the Δ-definition in this idealized flow containing helical vortex lines is important for proper identification of vortices with core size non-uniformity.

5.3.2. *Mixing layer*

We now consider DNS data of a temporal mixing layer, initialized with a hyperbolic tangent streamwise velocity profile and a sinusoidal spanwise distribution of streamwise vorticity, at the time of shear layer rollup (Park, Metcalfe & Hussain 1994). Figure 7(*a*) shows a very noisy vortex core boundary based on the Δ-definition in this flow, while the λ_2-definition (figure 7*b*) shows both the rib and roll vortical structures clearly. A contour plot of Δ in an (x, z)-plane between ribs reveals regions of both non-negligible Δ (denoted by A in figure 7*c*) and negligible Δ (denoted by B), which are excluded in the λ_2-definition (figure 7*d*). The noise in regions such as B may be eliminated by a slight increase of the Δ level, which, however, will not remove regions A. This implies that a significant portion of the small scales evident in Δ (figure 7*a*) is not due to numerical noise, which appears outside the roll. The $|\omega|$ surface and contours (figures 7*e*, *f*) are also smooth, confirming the lack of significant small scales; this is consistent with the smooth vortex core boundary given by the λ_2-definition.

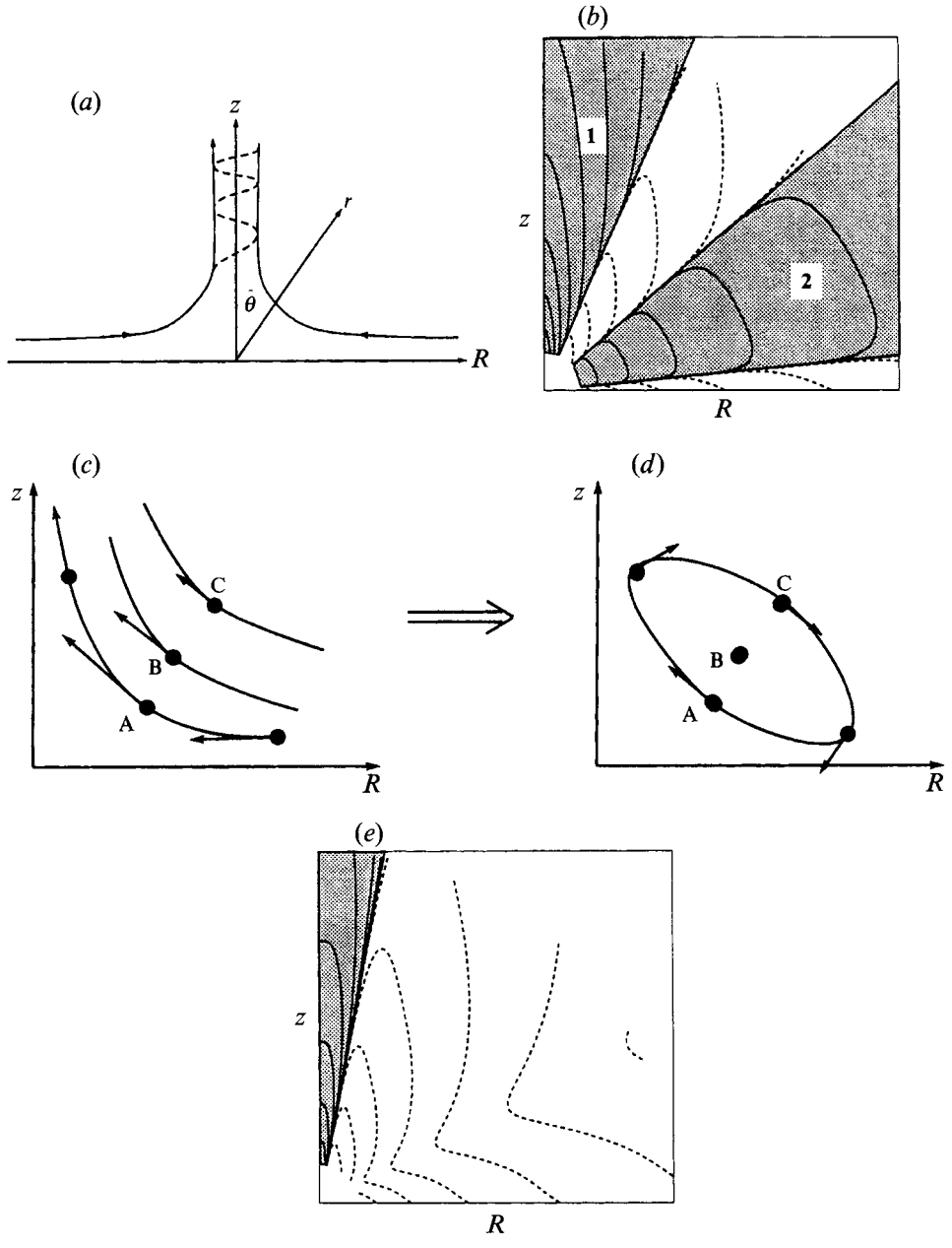

FIGURE 6. (*a*) Schematic of a swirling jet with conical symmetry. (*b*) Contours of Δ; regions of $\Delta > 0$ are marked by grey shading. (*c*, *d*) Schematics of streamline patterns in different reference frames. (*e*) Contours of $-\lambda_2$; region of $\lambda_2 < 0$ is marked by grey shading.

5.3.3. *Circular jet*

DNS data at the time of vortex sheet rollup (i.e. ring formation) from a temporally evolving circular jet with an initial top-hat velocity profile and random vorticity perturbation (Melander, Hussain & Basu 1991) is used here. The λ_2-definition also shows a well-defined vortical ring structure, as to be expected (figure 8*a*), while the Δ-definition overestimates the ring's core size and obscures its details (figure 8*b*). A

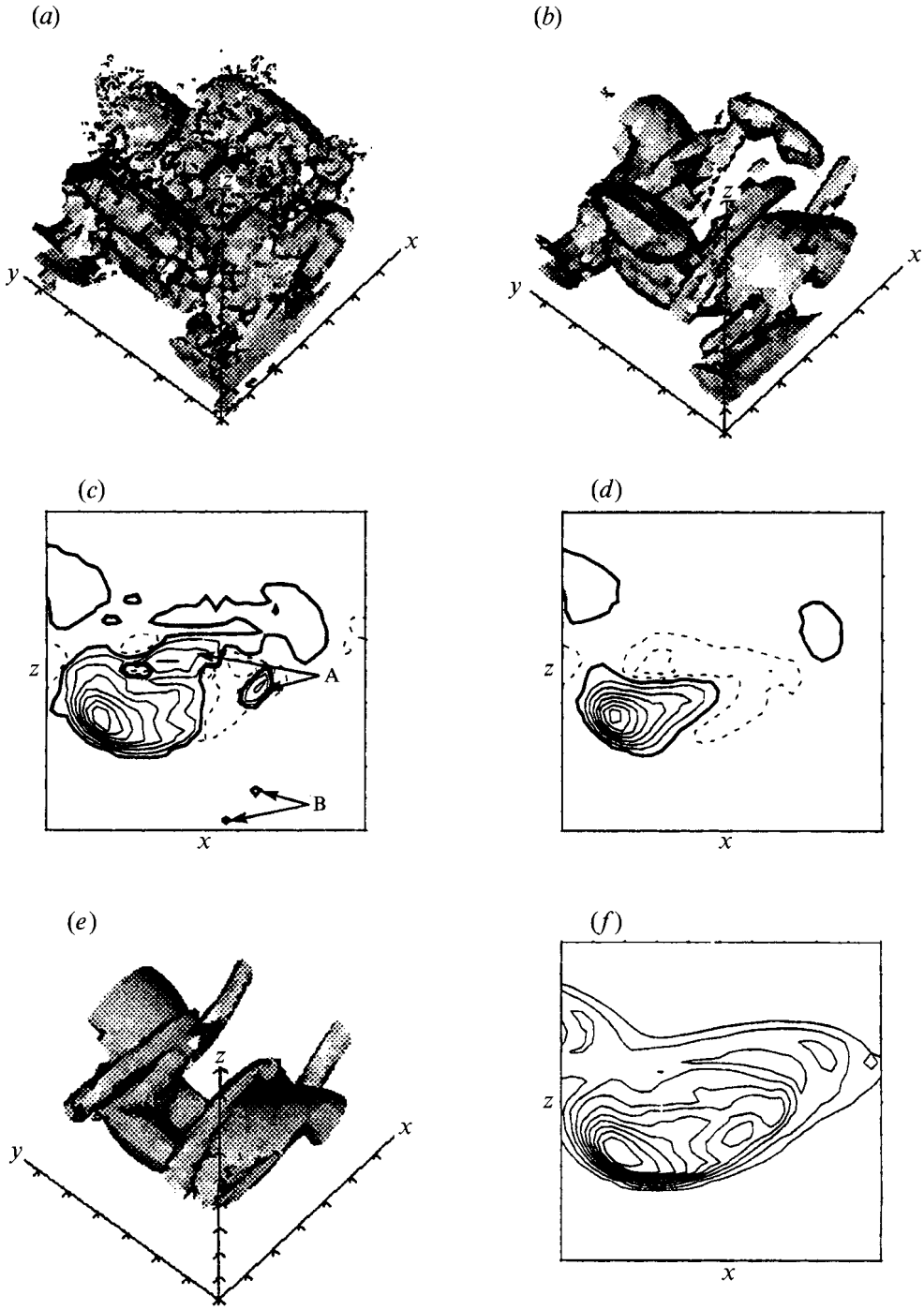

FIGURE 7. Plane mixing layer: (*a*) surface of $\Delta = 0$; (*b*) surface of $\lambda_2 = 0$. (*c*) Δ contours in an (x, z)-plane; (*d*) $-\lambda_2$ contours in an (x, z)-plane; (*e*) surface of $|\omega| = 25\%$ of maximum; (*f*) $|\omega|$ contours in an (x, z)-plane. Thick lines denote the boundary of the vortex cores.

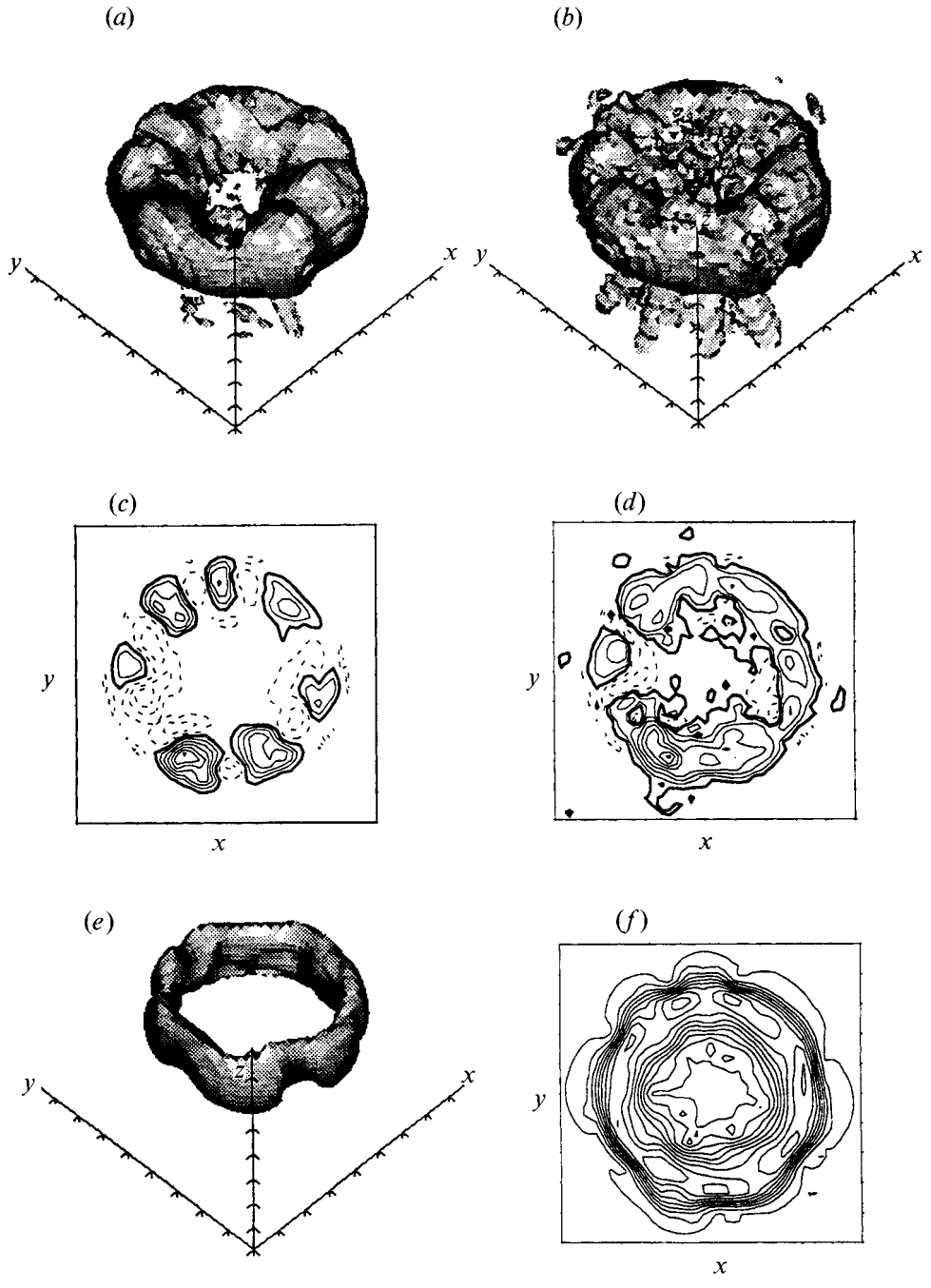

FIGURE 8. Circular jet: (*a*) surface of $\lambda_2 = 0$; (*b*) surface of $\Delta = 0$; (*c*) $-\lambda_2$ contours in an (x, y)-plane; (*d*) Δ contours in an (x, y)-plane; (*e*) surface of $|\omega| = 55\%$ of maximum; (*f*) $|\omega|$ contours in an (x, y)-plane. Thick lines denote the boundary of the vortex cores.

contour plot of $-\lambda_2$ in an (x, y)-plane near the bottom of the vortex ring (figure 8*c*) shows seven disjointed regions of the vortex core, while the Δ-definition shows only two such regions in the same plane (figure 8*d*). The positive values of Δ in the negative regions of $-\lambda_2$ are not negligible, showing that the Δ-definition clearly overestimates

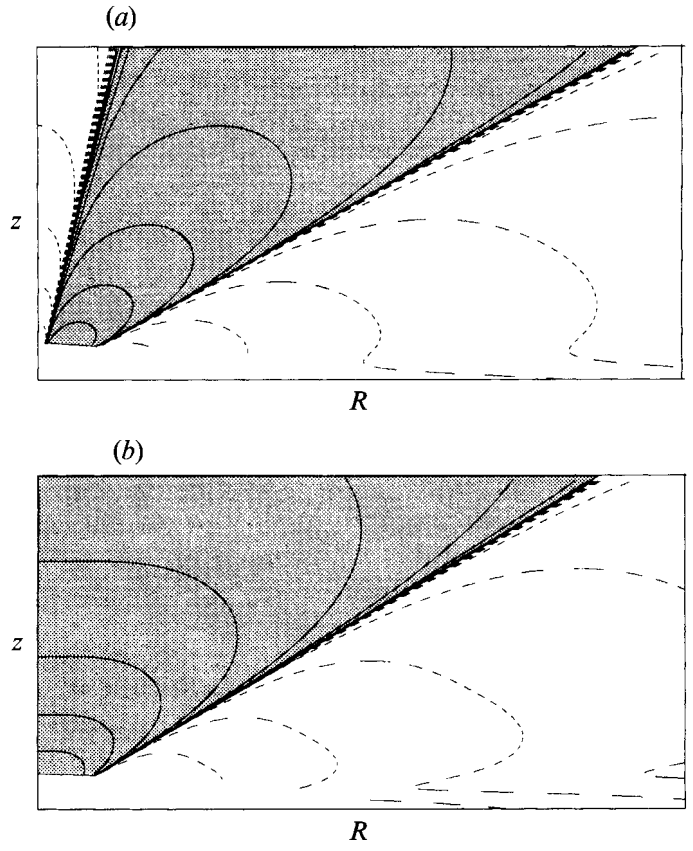

FIGURE 9. Contours of (*a*) Q and (*b*) $-\lambda_2$ in a swirling jet with conical symmetry; grey area denotes the region of $Q > 0$ and $\lambda_2 < 0$. Note that these figures cover only the near-axis region of the vortex in figure 6.

the vortex core in this flow. As for the mixing layer data, a slight increase of the Δ level does not remove the noisy boundary. For example, the next level in figure 8(*d*) is about 15% of the maximum value; an increase of the Δ contour level by 3% gives a similarly noisy vortex core boundary.

As in §5.3.2, the small scales of the vortex boundary defined by the Δ-definition are not due to small scales in the flow, as shown by the $|\omega|$ surface and contours (figures 8*e*, *f*). In summary, excessively noisy vortex core boundaries occur for the Δ-definition in DNS data, a difficulty not encountered with the λ_2-definition.

5.4. *Inadequacy of the Q-definition*

5.4.1. *Conically symmetric vortex*

For a description of this flow, see §5.3.1. Since Q is negative near the axis and becomes positive away from it, the Q-definition shows a narrow hollow core along the axis (figure 9*a*), as compared to the geometry given by the λ_2-definition (figure 9*b*); note that figure 9(*a*, *b*) covers only near-axis regions of the vortex in figure 6. This exclusion is unreasonable because fluid particles near the axis undergo nearly solid-body rotation. Thus, the Q-definition does not properly represent the vortex geometry, while the λ_2-definition reveals the vortex core geometry correctly, as shown earlier (figure 6*e*).

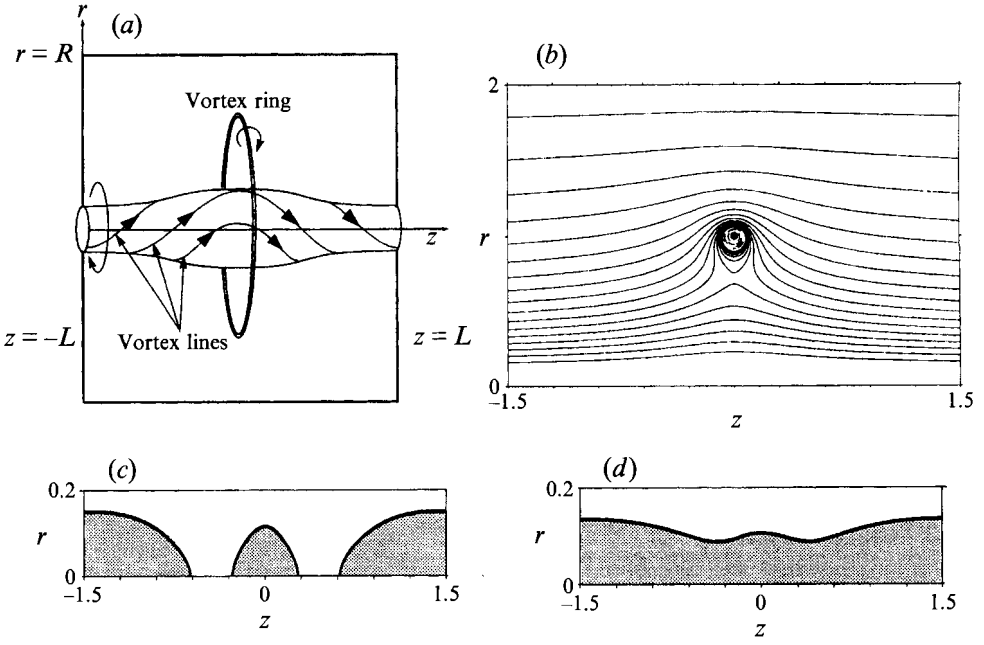

FIGURE 10. An axial vortex passing through the centre of a vortex ring: (*a*) schematic; (*b*) streamfunction; (*c*) $Q = 0$; and (*d*) $\lambda_2 = 0$.

5.4.2. *An axisymmetric axial vortex within a vortex ring*

We consider here an inviscid, steady axisymmetric axial vortex embedded in a thin vortex ring as shown in figure 10(*a*). A small core radius of the vortex ring, $l_r/L_r = 10^{-3}$, where l_r and L_r are the core radius of the vortex ring and the size of the domain in the radial direction, is used to avoid the large recirculation zone which otherwise appears on the axis (Batchelor 1967, p. 525). A computational box with an aspect ratio $L_r/L = 4/3$ and 400×400 grid points was used to obtain an inviscid steady solution. For the axial vortex, $u_\theta(r, z = -L)$, $\omega_\theta(r, z = -L)$ and axial velocity $u_z(r, z = \pm L)$ are given as

$$\left.\begin{aligned} \Gamma = ru_\theta(r, z = -L) &= \Gamma_0(1 - \exp(-(r/\delta)^2)), \\ \omega_\theta(r, z = -L) &= U_a r \exp(-(r/\delta)^2), \\ u_z(r, z = \pm L) &= U_b + U_a \exp(-(r/\delta)^2), \end{aligned}\right\} \tag{8}$$

where U_b is the propagation velocity of the vortex ring, and U_a is the axial velocity at the centre induced by ω_θ of the axial vortex. Γ and ω_θ at the inflow boundary are cut off at $r = 2\delta$ to make the axial vortex compact. The steady solution is obtained by solving a nonlinear elliptic equation (Batchelor 1967, p. 545):

$$\frac{\partial^2\psi}{\partial r^2} - \frac{1}{r}\frac{\partial\psi}{\partial r} + \frac{\partial^2\psi}{\partial z^2} = -r\omega_\theta = r^2\frac{\mathrm{d}H}{\mathrm{d}\psi} - \Gamma\frac{\mathrm{d}\Gamma}{\mathrm{d}\psi},$$

where $H = p/\rho + \frac{1}{2}v^2$ is the total head. From the above boundary conditions (8), the functional relations of Γ and H to ψ are obtained, and the nonlinear elliptic equation is solved iteratively.

The streamlines in a meridional plane show that the axial vortex maintains a local expansion due to the induced motion of the ring (figure 10*b*). The Q-definition

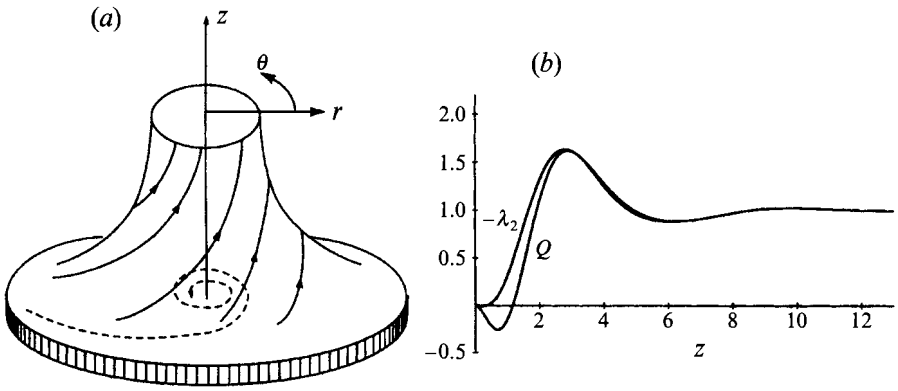

FIGURE 11. Bödewadt's vortex: (*a*) schematic; (*b*) distributions of λ_2 and Q.

incorrectly shows disconnected vortex cores (figure 10*c*) along the axis of the continuous axisymmetric vortex column, implying that the Q-definition becomes inadequate if a vortex expands locally due to an imposed non-uniform strain field. In contrast, the λ_2-definition correctly shows a continuous vortex core (figure 10*d*).

5.4.3. *Bödewadt vortex*

This flow is a vortex normal to a stationary wall with solid-body rotation (of angular velocity Ω) far from the wall (Bödewadt 1940); that is, this flow is the inverse of the Kármán vortex pump mentioned in §2.1. Away from the wall, the centrifugal force is balanced by the radial pressure gradient (cyclostrophic balance). However, the viscous effect decreases the azimuthal velocity near the wall, whereas the radial pressure gradient remains the same as that away from the wall. As a result of the decreased centrifugal force near the wall, the unbalanced pressure force moves fluid near the wall toward the vortex axis and, by continuity, the fluid near the axis moves away from the wall as shown in figure 11(*a*). The distance and velocity are non-dimensionalized by $(\nu/\Omega)^{1/2}$ and $(\nu\Omega)^{1/2}$ respectively, and the velocity and pressure fields are

$$u_r = rF(z), \quad u_\theta = rG(z), \quad u_z = H(z), \quad P = \tfrac{1}{2}r^2 + P_0(z).$$

In this case, Q is negative when $z < 1.16$ since the positive eigenvalue λ_1 of $\boldsymbol{S}^2 + \boldsymbol{\Omega}^2$ cancels the negative eigenvalues λ_2 and λ_3 (figure 11*b*). Since vortical motion exists for all $z > 0$, the negative value of Q near the wall indicates misrepresentation of the vortex core. Note that λ_2 is negative for all $z > 0$ and the λ_2-definition is valid for this flow.

5.5. *Comparison of the four definitions for DNS data*

Why the λ_2-definition is preferable has been demonstrated above in various examples where the geometry of the vortex core is known intuitively. So far, we have considered cases which show noticeable differences to accentuate inadequacies of definitions based on Δ, Q and $|\omega|$. Now, with the goal of comparing these definitions in flows of practical relevance, we apply all four definitions to data from three numerically simulated flows, where, unfortunately, *a priori* intuition of the geometry of vortex cores is less clear.

As the first example, we consider a tanh-profile temporal mixing layer excited with spanwise perturbations to induce rollup and pairing of rolls and three-dimensional oblique modes to produce ribs (Schoppa 1994). To show the evolution of the flow, $|\omega|$ contours are shown in figure 12(*a–c*) for three time instants at a fixed spanwise

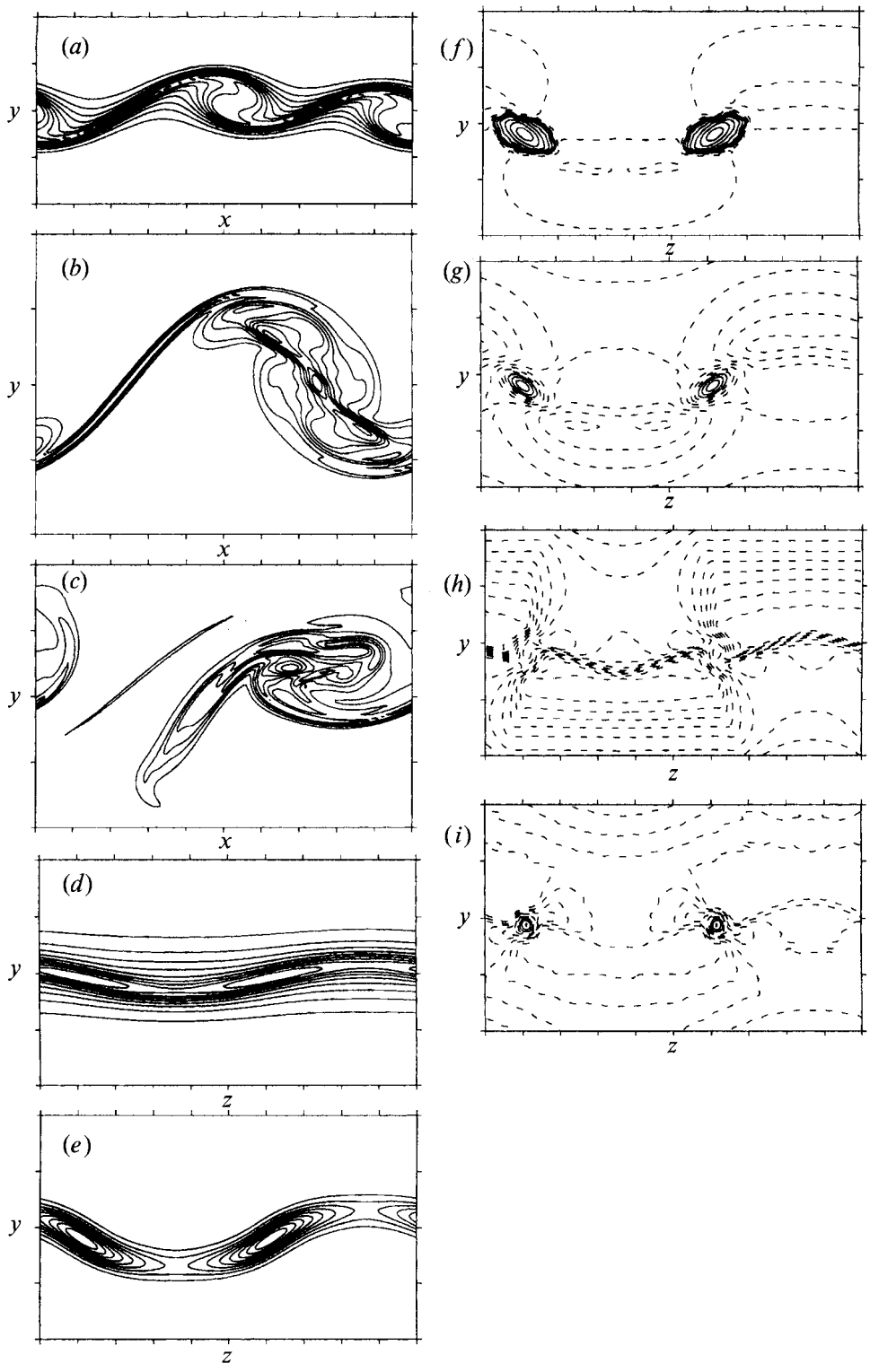

FIGURE 12. A temporally evolving mixing layer. (*a–c*) $|\omega|$ distribution in an (x, y)-plane halfway between two adjacent ribs: (*a*) during roll up; (*b*) during pairing; and (*c*) after pairing. (*d–i*)

location, halfway between two ribs. After the vortex sheet rolls up (corresponding to figure 12*a*), the vorticity magnitude in the braid shows local peaks (figure 12*d*), which suggest rib cores according to the $|\omega|$-definition. However, the other three definitions show no such vortex cores in the braid (not shown), suggesting that this vorticity sheet does not yet contain ribs (i.e. longitudinal vortices). Once pairing starts (figure 12*b*), local peaks in $|\omega|$ in a streamwise (i.e. y, z) plane through the braid centre become more pronounced (figure 12*e*). At this stage, Δ- and Q-definitions show the existence of ribs in the braid region (figure 12*f, g*). However, the λ_2-definition fails to identify these (figure 12*h*). As pairing continues (figure 12*c*), the accumulation of streamwise vorticity within ribs in the braid region intensifies. At this point, the local peaks of $|\omega|$ in the braid due to ribs are then recognized as vortex cores by the λ_2-definition (figure 12*i*). Thus, in contrast to λ_2-definition, Δ- and Q-definitions recognize ribs in the braid region while they are still ribbon-like (with elliptic cross-section) and well in advance of their 'collapse' into recognizable vortices with nearly circular cross-section.

As the second example, we consider the collision of two vortex rings which are initially oppositely polarized (this simulation was done by Dr D. Virk). The configuration of the two rings is the same as case III of Kida, Takaoka & Hussain (1991) except that, in the present case, the initial vortex rings are opposite polarized (i.e. vortex has a flow along the azimuthal direction in the core; these flows are such that the helical vortex lines in the core are right-handed in one vortex and left-handed in the other). A detailed description of the dynamics of a polarized ring appears in Virk, Melander & Hussain (1994). The time evolution of the vortex core boundary is shown using the $\lambda_2 = 0$ surface in figure 13(*a–d*). We consider a plane (marked as A–A′ in figure 13*d*) where the reconnected and original vortex cores are fused together. We apply all four definitions to this plane; the differences among the definitions are obvious from the contours in figure 13(*e–h*) drawn in the same spatial scales. The vortex core identified by the $|\omega|$-definition at any level (figure 13*e*) is significantly different from the boundary given by the λ_2-definition (figure 13*f*). The vortex core based on the Δ-definition (figure 13*g*) occupies a much larger area than that based on the λ_2-definition and shows noisy boundaries, as in §5.3. Figure 13(*h*) shows that the details of the vortex core boundary based on the Q-definition are slightly different from those based on the λ_2-definition.

As the final example, we consider the evolution of an axisymmetric column vortex with core size non-uniformity where strong core dynamics occurs (for details of core dynamics, see Melander & Hussain 1993). Initially, the circulation ru_θ at a fixed r is perturbed sinusoidally in the axial direction, and the distributions of the circulation and axial vorticity are shown in figures 14(*a, b*). Note that the axial velocity and azimuthal vorticity are initially zero everywhere, but emerge immediately as a result of core dynamics. The initial vortex core boundary identified by the λ_2-, Q-, and Δ-definitions corresponds to the radius where $\partial u_\theta/\partial r = 0$, and are the same, as shown in figure 14(*c*). Note that, as mentioned in §2.3, no $|\omega|$ isosurface matches the initial vortex core boundary identified by the λ_2-, Q-, and Δ-definitions.

The evolutions of vortex core boundaries (marked by a thick line) identified by the λ_2-, Δ-, and Q-definitions are shown in figure 14(*d–f*) for four instants (T_1–T_4) covering approximately a half-period of the evolution of the core dynamics cycle; the differences between the three definitions at each of the instants are clear. The vortex core identified by the λ_2-definition (figure 14*d*) clearly shows core deformation due to core dynamics.

Distributions in an (y, z)-plane cutting through the braid: (*d*) $|\omega|$ contours during roll up; (*e*) $|\omega|$ contours during pairing; (*f*) Δ contours during pairing; (*g*) Q contours during pairing; (*h*) $-\lambda_2$ contours during pairing; and (*i*) $-\lambda_2$ contours after pairing.

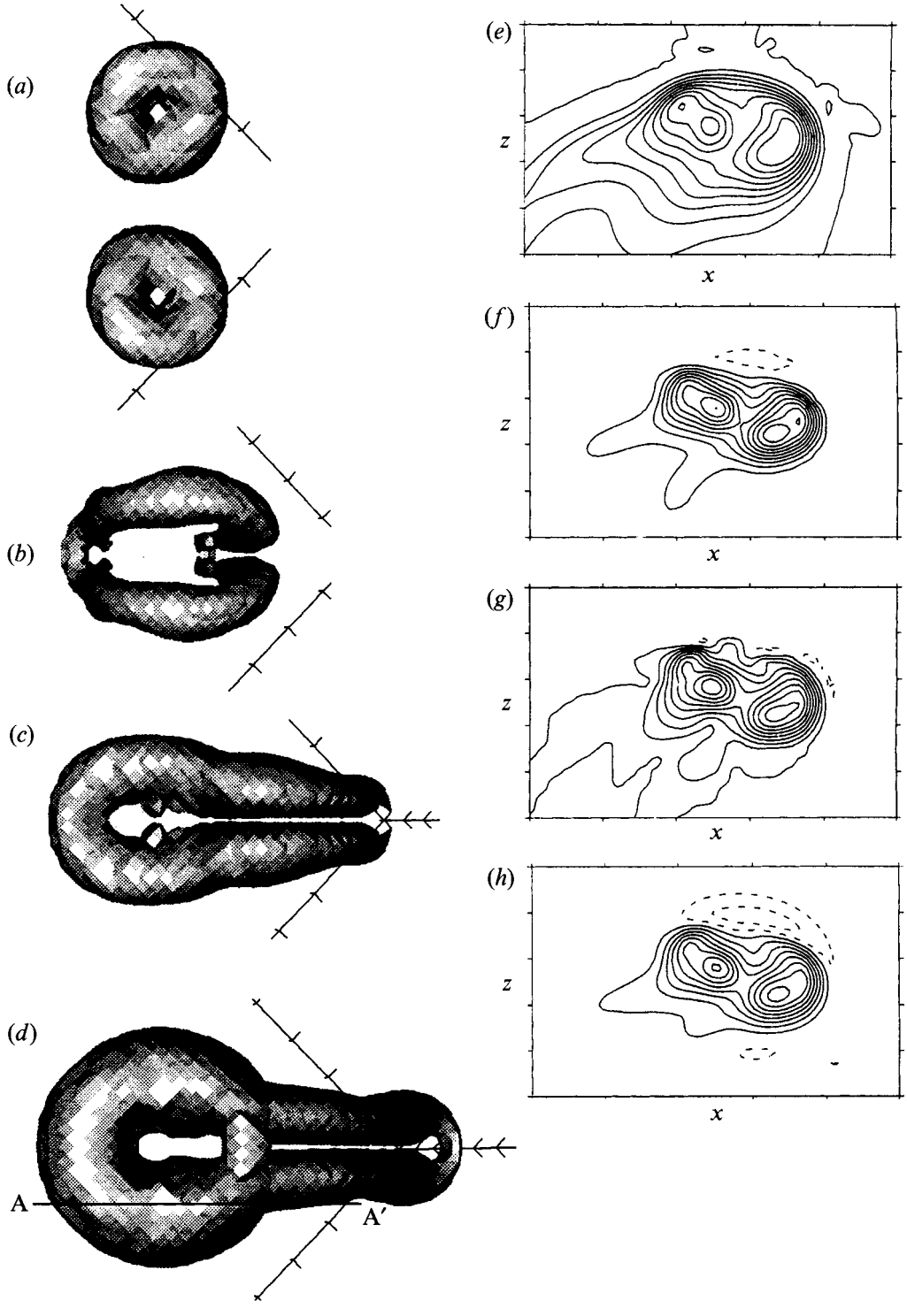

FIGURE 13. Collision of vortex rings with opposite polarities. (*a–d*) Evolution of the vortex core identified by the surface based on λ_2-definition. (*e–h*) Distributions through the plane A–A′ of: (*e*) $|\omega|$; (*f*) $-\lambda_2$; (*g*) Δ; and (*h*) Q.

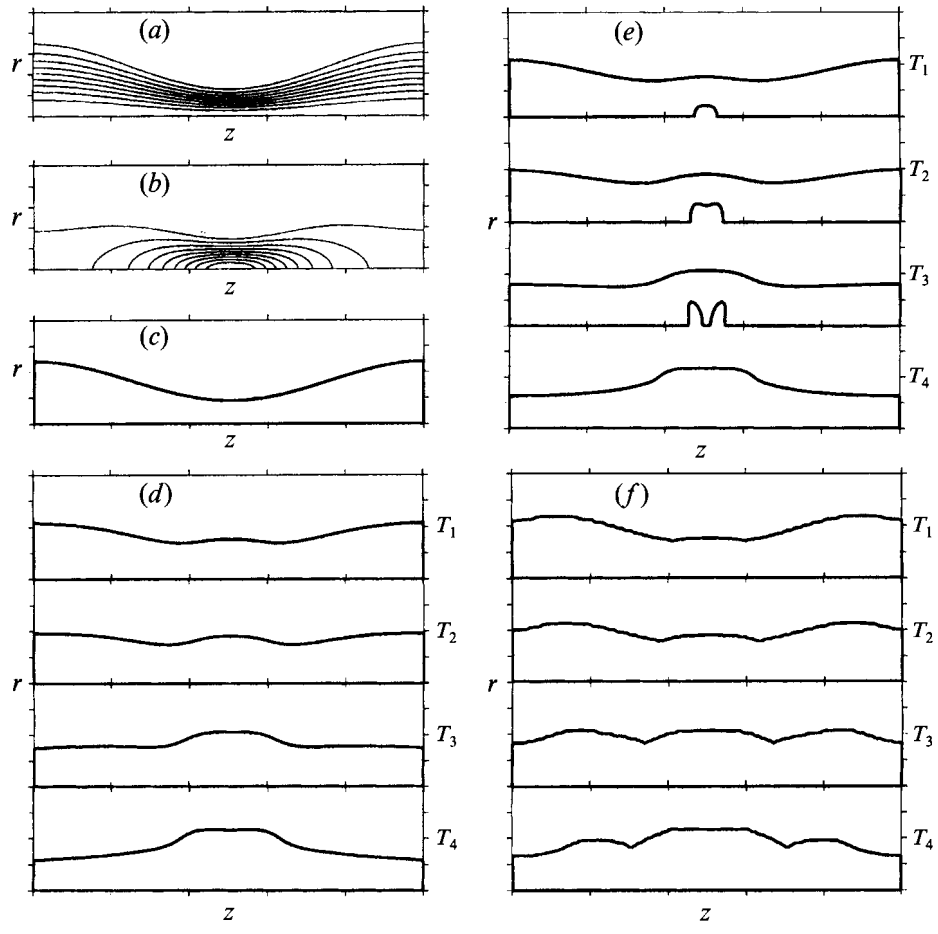

FIGURE 14. Evolution of an axial vortex with core non-uniformity in the meridional plane. (*a*, *b*) Initial distributions of: (*a*) ru_θ and (*b*) ω_z. (*c*) Initial vortex core boundary identified by λ_2-, Q-, and Δ-definitions. (*d–f*) Evolution of vortex core boundaries (at successive times T_1, T_2, T_3 and T_4) identified by: (*d*) λ_2-definition; (*e*) Q-definition; and (*f*) Δ-definition.

However, the one identified by the Q-definition shows localized (low-enstrophy) bubbles on the axis excluded from the vortex core (figure 14*e*); note the similarity to the cases shown in §5.4. The vortex core identified by the Δ-definition does not show a bubble on the axis, but it shows three waves (figure 14*f*) instead of the single wave shown in the λ_2-definition (figure 14*d*). The low-enstrophy bubbles are indeed intrinsic to core dynamics (Melander & Hussain 1993), but are also integral parts of the vortex core.

In summary, the Q- and λ_2-definitions tend to be similar but often differ from the Δ- and $|\omega|$-definitions; however, the Q- and λ_2-definitions show significant differences in regions where vortex stretching or compression are significant. Assuming that the λ_2-definition represents the underlying vortical structures more accurately than the other three definitions (based on data discussed in the previous sections), the evolution of connected negative λ_2 domains appears more appropriate for studying evolutionary dynamics and related flows physics of vortices and coherent structures.

6. Concluding remarks

Among the four definitions, only the λ_2-definition is found to represent the topology and geometry of vortex cores correctly for the large variety of flows considered in this paper. The λ_2-definition corresponds to the pressure minimum in a plane, when contributions of unsteady irrotational straining and viscous terms in the Navier–Stokes equations are discarded; this way, only the contribution of $\boldsymbol{S}^2+\boldsymbol{\Omega}^2$ to $p_{,ij}$ is taken into account. This is the underlying reason for the success of our λ_2-definition in representing the vortex core geometry correctly in unsteady and low-Re flows, while the definition based on the pressure minimum misrepresents the vortex core geometry in these and many other situations.

Recall that λ_2 is the median of the three eigenvalues of $\boldsymbol{S}^2+\boldsymbol{\Omega}^2$, and $Q = -\frac{1}{2}(\lambda_1+\lambda_2+\lambda_3)$. Although in most cases the Q- and λ_2-definitions result in similar vortex cores, they can be quite different, as shown to be so for an axisymmetric axial vortex within a vortex ring and a conically symmetric vortex with axial velocity. In the conically symmetric vortex, the Q-definition incorrectly shows a hollow core near the centre and hence misrepresents the vortex core in this case. For the axial vortex passing through a vortex ring, the vortex core based on the Q-definition is disconnected, implying that vortex identification by the Q-definition may be incorrect when vortices are subjected to a strong external strain. Thus, we expect problems with the Q-definition for vortices with strong core dynamics.

For DNS data, Δ tends to be slightly positive even outside the vortex cores. As a result, the Δ-definition has a noisy boundary which overestimates both the vortex core size and the predominance of small scales in the flow. For example, in a circular jet, the Δ-definition incorrectly shows one (singly connected) blob, instead of the actual vortex ring (with a hole). In addition, the Δ-definition shows a spurious detached vortex core in a conically symmetric vortex.

The $|\omega|$-definition does not have an *a priori* defined level, so that the vortex core boundaries based on this definition are ambiguous. For vortex cores embedded in a surrounding flow with a shear comparable to the vorticity within the core (e.g. wall-bounded and homogeneous shear flows), the maximum $|\omega|$ may be located outside the vortex core, causing even a high-level $|\omega|$ surface to misrepresent the vortex core.

Being a non-local variable, pressure has an inherently larger scale than the vortex core; hence, the scale of the vortex core is misrepresented by a pressure isosurface. For instance, the pressure within a rib in a mixing layer may have a value near that of the ambient. Thus, a pressure isosurface depicting the ribs may obsure both the rib and roll vortices.

Hussain (1986) defined a coherent structure in terms of vorticity as 'a coherent structure is a connected turbulent fluid mass with instantaneous phase-correlated vorticity over its spatial extent'. Since coherent structures are vortical, we suggest that coherent structures be defined as *domains of phase-correlated negative* λ_2 instead of phase-correlated vorticity.

We are grateful to Wade Schoppa and Nick Kevlahan for helpful comments and suggestions. This research was funded by the AFOSR grant F496620-92-J-0200 and the ONR grant N00014-89-J-1361.

REFERENCES

BATCHELOR, G. K. 1967 *Introduction to Fluid Dynamics*. Cambridge University Press.

BISSET, D. K., ANTONIA, R. A. & BROWNE, L. W. B. 1990 Spatial organization of large structures in the turbulent far wake of a cylinder. *J. Fluid Mech.* **218**, 439.

BLACKWELDER, R. F. 1977 On the role of phase information in conditional sampling. *Phys. Fluids* **20**, S232.

BÖDEWADT, U. T. 1940 Die Drehströmung über festern Grund. *Z. Angew. Math. Mech.* **20**, 141.

CANTWELL, B. J. 1981 Organized motion in turbulent flow. *Ann. Rev. Fluid Mech.* **13**, 457.

CANTWELL, B. J. & COLES, D. 1983 An experimental study of entrainment and transport in the turbulent near wake of a circular cylinder. *J. Fluid Mech.* **136**, 321.

CHONG, M. S., PERRY, A. E. & CANTWELL, B. J. 1990 A general classification of three-dimensional flow field. *Phys. Fluids* A **2**, 765.

COURANT, R. & HILBERT, D. 1953 *Methods of Mathematical Physics*, vol. 1. Interscience.

FERRÉ, J. A. & GIRALT, F. 1989 Pattern recognition analysis of the velocity field in plane turbulent wakes. *J. Fluid Mech.* **198**, 27.

FIEDLER, H. E. & MENSING, P. 1985 The plane turbulent shear layer with periodic excitation. *J. Fluid Mech.* **150**, 281.

HUNT, J. C. R. 1987 Vorticity and vortex dynamics in complex turbulent flows. In *Proc. CANCAM, Trans. Can. Soc. Mech. Engrs* **11**, 21.

HUNT, J. C. R., WRAY, A. A. & MOIN, P. 1988 Eddies, stream, and convergence zones in turbulent flows. *Center for Turbulence Research Report CTR*-S88, p. 193.

HUSAIN, H. S. & HUSSAIN, F. 1993 Elliptic jets. Part 3. Dynamics of preferred mode coherent structure. *J. Fluid Mech.* **248**, 315.

HUSSAIN, A. K. M. F. 1980 Coherent structures and studies of perturbed and unperturbed jets. In *The Role of Coherent Structures in Modelling Turbulence and Mixing* (ed. J. Jimenez) Lecture Notes in Physics, vol. 136, pp. 252–291. Springer.

HUSSAIN, F. 1986 Coherent structures and turbulence. *J. Fluid Mech.* **173**, 303.

HUSSAIN, A. K. M. F. & HAYAKAWA, M. 1987 Eduction of large-scale organized structure in a turbulent plane wake. *J. Fluid Mech.* **180**, 193.

HUSSAIN, F. & MELANDER, M. V. 1991 Understanding turbulence via vortex dynamics. In *The Lumley Symposium: Studies in Turbulence*, pp. 157–178. Springer.

HUSSAIN, A. K. M. F. & ZAMAN, K. B. M. Q. 1980 Vortex pairing in a circular jet under controlled excitation. Part 2. Coherent structure dynamics. *J. Fluid Mech.* **101**, 493.

JEONG, J. 1994 A theoretical and numerical study of coherent structures. PhD dissertation, University of Houston.

JIMENEZ, J., MOIN, P., MOSER, R. & KEEFE, L. 1988 Ejection mechanisms in the sublayer of a turbulent channel. *Phys. Fluids* **31**, 1311.

KIDA, S., TAKAOKA, M. & HUSSAIN, F. 1991 Collision of two vortex rings. *J. Fluid Mech.* **230**, 583.

KIM, J. 1985 Turbulence structures associated with the bursting event. *Phys. Fluids.* **28**, 52.

LAMB, H. 1945 *Hydrodynamics*. Dover.

LUMLEY, J. L. 1981 Coherent structures in turbulence. In *Transition and turbulence* (ed. R. E. Meyer), pp. 215–242. Academic.

LUGT, H. J. 1979 The dilemma of defining a vortex. In *Recent Developments in Theoretical and Experimental Fluid Mechanics* (ed. U. Müller, K. G. Roesner & B. Schmidt), pp. 309–321. Springer.

MELANDER, M. V. & HUSSAIN, F. 1988 Cut-and-connect of two antiparallel vortex tubes. *Center for Turbulence Research Rep. CTR*-S88, pp. 257–286.

MELANDER, M. & HUSSAIN, F. 1993 Polarized vorticity dynamics on a vortex column. *Phys. Fluids* A **5**, 1992.

MELANDER, M. V., HUSSAIN, F. & BASU, A. 1991 Breakdown of a circular jet into turbulence. In *Turbulent Shear Flows 8, Munich*, pp. 15.5.1–15.5.6.

METCALFE, R. W., HUSSAIN, F., MENON, S. & HAYAKAWA, M. 1985 Coherent structures in a turbulent mixing layer: a comparison between numerical simulations and experiments. In

Turbulent Shear Flows 5 (ed. F. Durst, B. E. Launder, J. L. Lumley, F. W. Schmidt & J. H. Whitelaw), p. 110. Springer.

MOFFATT, H. K. 1963 Viscous and resistive eddies near a sharp corner. *J. Fluid Mech.* **18**, 1.

MUMFORD, J. C. 1982 The structures of the large eddies in fully developed turbulent shear flows. Part 1. The plane jet. *J. Fluid Mech.* **118**, 241.

PANTON, R. L. 1984 *Incompressible Flow*. Wiley.

PARK, K., METCALFE, R. W. & HUSSAIN, F. 1994 Role of coherent structures in an isothermally reacting mixing layer. *Phys. Fluids* **6**, 885.

ROBINSON, S. K. 1991 The kinetics of turbulent boundary layer structure. PhD Dissertation, Stanford University.

SCHOPPA, W. 1994 A new mechanism of small-scale transition in a plane mixing layer: core dynamics of spanwise vortices. MS thesis, University of Houston.

SCHOPPA, W., HUSAIN, H. & HUSSAIN, F. 1993 Nonlinear instability of free shear layers: subharmonic resonance and three-dimensional vortex dynamics. *IUTAM Symp on Nonlinear Instability of Nonparallel Flows* (ed. S. P. Lin *et al.*), *26–30 July, 1993, Clarkson University*, pp. 251–280.

SHTERN, V. & HUSSAIN, F. 1993 Hysteresis in a swirling jet as a model tornado. *Phys. Fluids* A **5**, 2183.

TENNEKES, T. & LUMLEY, J. L. 1972 *A First Course in Turbulence*. MIT Press.

TRUESDELL, C. 1953 *The Kinematics of Vorticity*. Indiana University.

TSO, J. 1983 Coherent structures in a fully-developed turbulent axisymmetric jet. PhD dissertation, Johns Hopkins University.

TSO, J. & HUSSAIN, F. 1989 Organized motions in a fully developed turbulent axisymmetric jet. *J. Fluid Mech.* **203**, 425.

VIRK, D., MELANDER, M. V. & HUSSAIN, F. 1994 Dynamics of a polarized vortex ring. *J. Fluid Mech.* **260**, 23.